©Operative Dentistry, 2019, **44-5,** 499-509

The Combination of CQ-amine and TPO Increases the Polymerization Shrinkage Stress and Does Not Improve the Depth of Cure of Bulk-fill Composites

MG Rocha • DCRS de Oliveira • MAC Sinhoreti • JF Roulet • AB Correr

Clinical Relevance

The combination of camphorquinone with violet absorption alternative photoinitiators does not improve the depth of cure and, consequently, can increase the polymerization shrinkage stress of bulk-fill composites.

SUMMARY

Objectives: To evaluate the effect of combining camphorquinone (CQ) and diphenyl(2,4,6-trimethylbenzoyl)phosphine oxide (TPO) on the depth of cure and polymerization shrinkage stress of bulk-fill composites.

Methods and Materials: Experimental bulk-fill composites were produced containing equal molar concentrations of either CQ-amine or CQ-amine/TPO. The degree of in-depth conversion through each millimeter of a 4-mm-thick bulk-fill increment was evaluated by Fourier transform near-infrared microspectroscopy using a central longitudinal cross section of the increment of each bulk-fill composite (n=3). Light-transmittance of the multi-wave light-emitting diode (LED) emittance used for photoactivation (Bluephase G2, Ivoclar Vivadent) was recorded through every millimeter of each bulk-fill composite using spectrophotometry. The volumetric shrinkage and polymerization shrinkage stress were assessed

†Mateus Garcia Rocha, DDS, MS, Department of Restorative Dentistry, Piracicaba Dental School, State University of Campinas, Piracicaba, São Paulo, Brazil

*†Dayane Carvalho Ramos Salles de Oliveira, DDS, MS, PhD, Department of Restorative Dentistry, Piracicaba Dental School, State University of Campinas, Piracicaba, São Paulo, Brazil

Mario Alexandre Coelho Sinhoreti, DDS, MS, PhD, Department of Restorative Dentistry, Piracicaba Dental School, State University of Campinas, Piracicaba, São Paulo, Brazil

Jean-François Roulet, DDS, PhD Department of Restorative Dental Science, College of Dentistry, University of Florida, Gainesville, FL, USA

Americo Bortolazzo Correr, DDS, MS, PhD, Department of Restorative Dentistry, Piracicaba Dental School, State University of Campinas, Piracicaba, São Paulo, Brazil

*Corresponding author: 1395 Center Drive, Gainesville, FL, 32610, USA; e-mail: oliveira.day@icloud.com

†These authors contributed to conception, design, data acquisition, and analysis as well as drafted and critically revised the manuscript.

DOI: https://doi.org/10.2341/18-234-L

using a mercury dilatometer and the Bioman, respectively. The flexural modulus was also assessed by a three-point bend test as a complementary test. Data were analyzed according to the different experimental designs (α=0.05 and β=0.2).

Results: Up to 1 mm in depth, adding TPO to CQ-based bulk-fill composites increased the degree of conversion, but beyond 1 mm no differences were found. The light-transmittance of either wavelengths emitted from the multi-wave LED (blue or violet) through the bulk-fill composites were only different up to 1 mm in depth, regardless of the photoinitiator system. Adding TPO to CQ-based bulk-fill composites did not affect volumetric shrinkage but did increase the flexural modulus and polymerization shrinkage stress.

Conclusion: Adding TPO to CQ-based bulk-fill composites did not increase the depth of cure. However, it did increase the degree of conversion on the top of the restoration, increasing the polymerization shrinkage stress.

INTRODUCTION

Bulk-fill composites (BFCs) are light-cured, resin-based materials used for the direct restorations of posterior teeth that can be placed in increments up to 4 to 5 mm thick.[1] The higher depth of cure of these composites in comparison to regular resin composites can be related not only to modifications in their monomers and filler compositions but also in the photoinitiator system used. As an example, some manufacturers use some alternative photoinitiators, such as diphenyl (2,4,6-trimethylbenzoyl) phosphine oxide (TPO) and benzoyl germanium (Ivocerin) in combination with camphorquinone (CQ), claiming that this combination improves the depth of cure.[2-4]

One possible explanation is that these alternative photoinitiators are more reactive than CQ, and they also produce more free radicals capable of initiating the polymerization, thus increasing the degree of conversion.[5] However, these alternative photoinitiators generally absorb violet light, which has a lower transmittance compared with blue light; thus, they might increase the degree of conversion only on the top of the restoration and might not increase the depth of cure of composites.[6] While monomers (type and size), fillers (load and size), and pigments might act as competitive absorptive components for both violet and blue light transmission throughout resin-based materials, it remains unclear whether the photoinitiator system absorption as an isolated factor has a significant effect on BFC light transmission and depth of cure. One question that needs to be asked is whether the increase in degree of conversion on the top would move the refractive index of the polymer formed closer to that of the filler used.[7,8] This would reduce the mismatch between the resin and filler refractive indexes, improving the transmission of blue light to the deeper portions of the restoration, thus enhancing free-radical formation by the CQ-amine photoinitiator system at the bottom part of the restoration. This would then increase the depth of cure as claimed.

On the other hand, *in vitro* studies have shown that BFC restorations might fail due to internal gap formations or by enamel cracks formed in nearby restoration margins,[9] possibly correlated to the polymerization shrinkage stress of the composite bulk.[10] Moreover, clinical evidence has shown that BFCs containing CQ-amine combined with TPO had worse clinical performance than BFCs containing only CQ-amine as the photoinitiator system. Interestingly, what is striking in the study of Bayraktar and others[11] is that CQ-amine combined with TPO showed more incidence of discontinued anatomic form, marginal discoloration, crevices in which dentin was exposed, and secondary caries in just one year of observation. Therefore, it is possible that the combination of these photoinitiators might not only improve the depth of cure but also play a role in the polymerization shrinkage stress of BFCs with a given resin/filler configuration.

Thus, the aim of this study was to evaluate the effect of combining TPO and CQ on the depth of cure and shrinkage stress of BFCs. The tested hypotheses were that 1) the combination of CQ and TPO will increase the depth of cure of BFCs and that 2) the combination of CQ and TPO will increase the polymerization shrinkage stress of BFCs.

METHODS AND MATERIALS

BFC Formulation

The monomers and filler particles used in the BFC formulation are listed in Table 1. This formulation is based on a BFC formulation patent[12] that has monomers and filler particles with refractive indexes very similar to each other (n=1.518 for uncured resin monomer blend; n=1.549 for cured resin monomer blend; and n=1.553 for the 7.5 μm $BaBSiO_2$ filler). This reduces light scattering inside the composite, which better identifies the effect of light transmission throughout the BFC.[7,13,14]

Table 1: *Chemical Products Used in Bulk-fill Composite Composition*

Material	Chemical	Refractive Index	Concentration (wt%)	Manufacturer
Monomer	Bis-EMA	1.535	16.10	Sigma Aldrich, St Louis, MO, USA.
Monomer	Exothane 24	1.4853	5.75	Esstech Inc, Essington, PA, USA.
Monomer	TEGDMA	1.483	1.15	Sigma Aldrich, St Louis, MO, USA.
Filler particle	16 nm fumed silica	1.535	2	Evonik Industries AG, Essen, Germany.
Filler particle	7.5 μm $BaBSiO_2$	1.553	75	Esstech Inc, Essington, PA, USA.

Abbreviations: $BaBSiO_2$, barium borosilicate; Bis-EMA, ethoxylated bisphenol A diglycidyldimethacrylate; TEGDMA, triethylene glycol dimethacrylate.

First, the monomers were blended using a centrifugal mixing device (SpeedMixer, DAC 150.1 FVZ-K, Hauschild Engineering, Hamm, North Rhine-Westphalia, Germany) for 60 seconds at 3000 rpm. To this monomer blend, two different photoinitiator systems were used, as shown in Table 2. The molar ratio concentration of CQ-amine and CQ-amine/TPO were based on previous studies.[15]

Then, the fumed silica filler was mixed with the monomer blend for 30 seconds at 3000 rpm followed by the $BaBSiO_2$ filler for 1 minute at 3500 rpm. Finally, each resin composite was mixed for 1 minute at 3500 rpm under an 80 mmHg vacuum atmosphere.

Light-Curing Unit Characterization

The mean irradiance (mW/cm^2) of the multi-wave light-emitting diode (LED; Bluephase G2, Ivoclar Vivadent, Schaan, Liechtenstein) was measured five times using a portable spectrometer-based instrument (CheckMARC, BlueLight Analytics, Halifax, Nova Scotia, Canada) connected to the SpectraSuite software (Spectra Suite 2.0.140, Ocean Optics, Dunedin, FL, USA). The total spectral radiant power output from the LED was divided by the cross-sectional active area (cm^2) of the light tip to calculate the average irradiance (mW/cm^2). These values were used to calculate the photoactivation time needed to produce a radiant exposure of 20 J/cm^2. Then, the multi-wave LED was attached to an x-y-z positioning device mounted on an optical bench to standardize the positioning of the light beam in contact with a diffusive surface of a frosted diffuser target (DG20-1500, Thorlabs, Inc, Newton, NJ, USA) while the resulting image was recorded using a CMOS camera (NEX-F3, Sony Corporation, Tokyo, Japan) with a 50-mm focal length lens. To assess the irradiance distribution at different light emission wavelengths, the CMOS camera beam profiler was used with the addition of bandpass filters (Thorlabs, Inc) placed in front of the camera lens. The bandpass filters were as follows: centered at 400 nm with a 4-nm full width at half maximum (FB400-40) was used to identify the LED chips with spectrum emission peaks at 410 nm and centered at 460 nm with a 10-nm full width at half maximum (FB460-10) was used to identify the LED chips generating emission peaks near 460 nm. As the bandpass filters used in this study have an optical density of approximately 0.2, no neutral density filters were necessary to attenuate the multi-wave LED emission to avoid pixel intensity saturation in the images. To produce calibrated images and data showing the irradiance patterns across the surface of the multi-wave LED, the mean power values, obtained using the CheckMARC were entered into an open source optical analysis software (Fiji, Nature Methods, National Institutes of Health, Bethesda, MD, USA). The scaled numeric data associated with each image was exported into a computer graphic software (Origin Pro, OriginLab Co, Northampton, MA, USA).

Table 2: *Photoinitiator Systems Used in the Bulk-fill Resin Composites*

Photoinitiator Systems	Molar ratio CQ:TPO	Concentration (wt%)		
		CQ	EDMAB	TPO
CQ-amine	1:0	0.50	0.58	0
CQ-amine/TPO	1:1	0.25	0.29	0.52

Abbreviations: CQ, camphorquinone; EDMAB, ethyl 4(dimethylamino) benzoate; TPO, diphenyl(2,4,6-trimethylbenzoyl) phosphine oxide.

Degree of Conversion (DC) in Width and Depth

Each BFC (n=3) was placed in a cylindrical Delrin acetal homopolymer resin mold (12 mm in height, 4 mm in inner diameter) with a Mylar strip manually pressed over the applied material with a glass plate to obtain a flat surface. Afterward, the glass plate was removed and the light curing was performed on the top of the cylinder using the multi-wave LED with 20 J/cm^2. Then, after 24 hours of dark and dry storage at 37°C, specimens ($12 \times 4 \times 0.5$ mm) were obtained by sections from the center of the specimen, perpendicular to the top surface and parallel to the long axis of the cylinder, using an automated water-cooled, low-speed diamond saw (Isomet 1000,

Buehler Ltd, Lake Bluff, IL, USA)[6,15,16] with temperature being monitored and recorded during cutting using a IR-Thermal Camera (FLIR Pro, FLIR, Wilsonville, OR, USA). The samples were not submitted to more than 3°C of increase in temperature.

The specimens were fixed onto a glass slab and placed over an automated x-y axis microscope platform. The DC was mapped along the cross section (width 6 mm; depth 4 mm) using a Fourier transform near-infrared (FT-NIR) microscope (Nicolet Continuum, Thermo Scientific, Waltham, MA, USA) coupled to an FT-NIR spectrometer (Nicolet Nexus 6700, Thermo Scientific).[6,15,17] Every 0.5 mm in depth and width, five infrared spectra were collected from the specimen. The measurements started from 300 μm below the top surface to avoid the area of oxygen inhibition. At each measurement position, the specimens' near-infrared spectra were collected in transmission mode with an aperture of 50 μm, 50 scans/spectrum, and 4 cm^{-1} of resolution. FT-NIR readings were performed in the transmission mode rather than the reflection mode to evaluate DC in bulk rather than on the surface of the material, which reduces the influence of monomer elution from the surfaces of the section specimens. The spectra of the uncured specimens (n=3) collected with the same settings were used as a reference to measure the peak area ratio corresponding to the aromatic double bonds (4625 cm^{-1}) and vinyl (6165 cm^{-1}) stretching absorptions. The DC (in %) was calculated as follows:

$$DC = \left[1 - \left(\frac{(\text{vinyl peak area}/\text{aromatic peak area})\text{pol}}{(\text{vinyl peak area}/\text{aromatic peak area})\text{non} - \text{pol}}\right)\right] \times 100,$$

where pol and non-pol correspond to the area of the methacrylate peak for the polymeric and monomeric states, respectively.

The results were exported to create color-coded maps to describe DC as a function of position in width and depth under the LED emission position using a computer graphic software (Origin Pro, OriginLab Co, Northampton, MA, USA). Each data point registered on the map was the average of three different replications using similar testing conditions. The map scales were set to indicate the maximum DC achieved and a reduction of 10% of the maximum DC in each subsequent color-coded area; a black dashed line was also drawn to represent the limit boundary of 80% of the maximum DC achieved by the BFCs.

Light Transmittance (LT)

The multi-wave LED spectral irradiance (mW/cm^2/nm) was obtained with a spectrophotometer (MARC Resin Calibrator, BlueLight Analytics) that has an optical fiber coupled to a cosine corrector sensor of Ø=3.9 mm and a field of view of 180°. The equipment was pre-calibrated using a traceable light source (LS-1-CAL, Ocean Optics) according to the standards of the National Institute of Standards and Technology (NIST, Gaithersburg, MD, USA). A spectroscopy software (Spectrasuite 2.0, Ocean Optics) was used to obtain the multi-wave LED spectral irradiance over a 380-495 nm wavelength range with a time acquisition of 20 seconds. The graphs obtained were used to calculate the spectral irradiance and the radiant exposure (J/cm^2) in the violet range (380-420 nm) and blue range (420-495 nm) by integrating the irradiance versus the wavelength in the spectral irradiance graphs.

LT through each BFC was recorded during the light curing using the same MARC Resin Calibrator spectrophotometer with the same parameters. Samples of each BFC (n=5) were placed in Delrin acetal homopolymer resin molds (Ø=4 mm) of different thicknesses (1 mm, 2 mm, 3 mm, 4 mm, 5 mm, and 6 mm) and positioned on the cosine corrector with Mylar strips covering the top and bottom surfaces of the samples. The spectral radiant power and the irradiance transmitted through each BFC were measured using the spectroscopy software. The spectral irradiance transmitted in the violet and blue ranges were determined for each BFC in different thicknesses. As LT is defined as the percentage of incident light that passes all the way through to the other side of the sample, LT in percent was calculated by subtracting the irradiance obtained at the bottom of each sample from the irradiance of the multi-wave LED in each wavelength range.

Volumetric Shrinkage (VS), Polymerization Shrinkage Stress (PSS), and Flexural Modulus (FM)

VS was measured using a mercury dilatometer (American Dental Association Health Foundation, Gaithersburg, MD, USA).[18] Approximately 0.1 g of each BFC (n=3) was placed on a sandblasted and silanized glass slide (75×25×1 mm). As the glass slide used was 1 mm thick and could attenuate the light that reaches the BFCs during light curing, before starting the test the multi-wave LED was recalibrated to deliver the same radiant exposure (20 J/cm^2) through the glass slide. After that, a glass

column was clamped to the glass slide, filled with mercury, and a linear variable differential transducer probe was placed on top of the mercury. VS was monitored for 60 minutes after the photoactivation. The data recorded by the probe was used to calculate the VS using previously measured mass and density values of BFCs.

PSS was measured for 600 seconds using the Bioman.[19] The BFCs were placed between a silanized glass slab and a roughened steel piston. The distance between the glass slab and the steel piston produced a 1-mm-thick composite that corresponded to a configuration factor of 5. The composites were photoactivated through the glass using the multi-wave LED with the same parameters used for the VS test. The load signal in Newton (N) was acquired and then divided by the disk area of the piston to obtain the maximum PSS values (MPa) and the maximum rate of PSS (rPSS, in $MPa.s^{-1}$).[20]

As the flexural modulus of the composite is correlated with the magnitude of the polymerization shrinkage stress, the FM was measured using a three-point bend test. Bar-shaped specimens of $10 \times 1 \times 1$ mm (n=10) were made in stainless steel molds. The specimen size of 1-mm thick was chosen according to previous studies to better evaluate mechanical properties.[21] The bulk increment was light-cured through a Mylar strip using the multi-wave LED with two light irradiations of 20 J/cm^2, overlapping each other by half of the diameter of the curing light tip. After 24 hours of storage in distilled water at 37°C, the specimens were submitted to a three-point bending test (Instron, Canton, MA, USA) at a crosshead speed of 0.75 mm/min until failure. FM was calculated in gigapascals (GPa) according to the following equation:

$$\mathrm{FM} = \frac{L \times D^3}{4 \times w \times h^3 \times d} \times 10^{-3},$$

where L = the maximum load at failure (N), D = distance between the supports, w = the specimen width, h = the specimen height, and d = crosshead displacement.

Statistical Analyses

Data were entered into statistical analysis software (Stata/MP 13, StataCorp, College Station, TX, USA) and checked for normality using the Shapiro-Wilks test and for variance homoscedasticity using the Levene test. Statistical analyses were performed according to the different experimental designs with a level of significance of $\alpha = 0.05$. A power analysis was conducted to determine the sample size for each experiment to provide a power of at least 0.8 at a significance level of 0.5 (β=0.2). DC was analyzed using a split-plot analysis of variance (ANOVA) where the independent variables were set as between-subject groups for the experimental BFC (CQ-amine or CQ-amine/TPO) and as within-subject groups for widths (0, 1, 2, 3, and 4 mm) and the depths (0, 1, 2, 3, and 4 mm). LTs in violet and blue range were analyzed independently using a two-way ANOVA where independent variables were set as BFC (CQ-amine or CQ-amine/TPO) and thicknesses (0, 1, 2, 3, 4, 5, and 6 mm). For DC and LT, the Tukey test was applied for multiple comparisons between groups (α=0.05). VS, PSS, rPSS, and FM were analyzed using a one-way ANOVA where independent variables were set as BFC (CQ-amine or CQ-amine/TPO).

RESULTS

The multi-wave LED provided a mean irradiance of 1151 ± 50 mW/cm^2 during the 17 seconds of exposure time, thus producing 20 ± 0.5 J/cm^2 of radiant exposure. However, 3.4 ± 0.2 J/cm^2 was within the violet wavelength range (380-420 nm) and 16.6 ± 0.4 J/cm^2 was within the blue range (420-540 nm) as represented in Figure 1A. Figure 1B,C shows the beam profile of the multi-wave LED according to the violet (380-420 nm) and blue (420-495 nm) wavelength range. The multi-wave LED had an active area of emission of 0.649 cm^2 and a maximum irradiance of 1386 mW/cm^2, but the irradiance and the wavelengths were not uniformly distributed across the light tip. In the black dashed circle area referenced to the size of the specimen, the multi-wave LED had an overall irradiance of 1025 mW/cm^2, where 152 mW/cm^2 was within the violet wavelength range (380-420 nm) and 873 mW/cm^2 was within the blue wavelength range (420-495 nm).

Table 3 shows the results of LT into the violet and the blue wavelength ranges for the CQ-amine and CQ-amine/TPO BFCs according to the different thicknesses. For both BFCs, there was an exponential decrease in LT as the specimen's thickness increased, regardless of the wavelength range. However, the CQ-amine BFC had a higher violet light transmittance than the CQ-amine/TPO BFC up to 1 mm in depth, but no differences were found beyond the 1-mm thickness. On the other hand, the CQ-amine/TPO BFC had a higher blue light transmittance than the CQ-amine up to 1 mm in depth, but no differences were found beyond the 1-mm thickness.

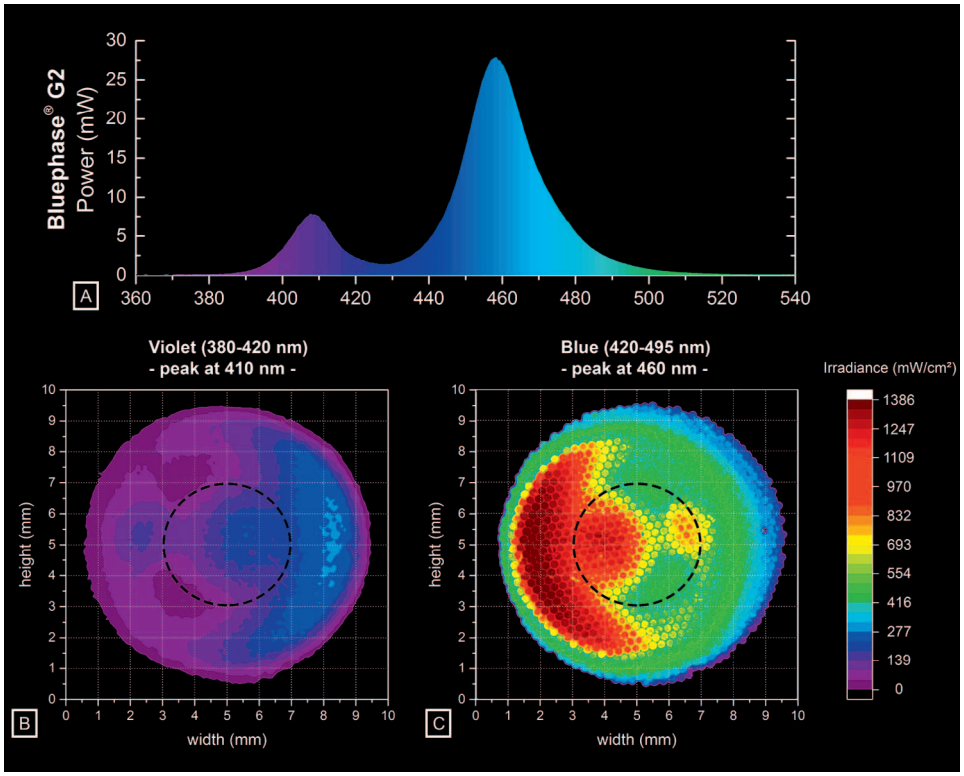

Figure 1. *(A) Graph representing the power (mW) versus the wavelength (nm) of the multi-wave LED (Bluephase G2) with a cumulative energy of 20 ± 0.5 J/cm² of radiant exposure. (B) Beam profile of the multi-wave LED with the 400 ± 40 nm bandpass filter showing the spectral emission pattern within the violet wavelength range (380-420 nm). The black dashed circle area (----) represents the position, orientation, and area of the specimen onto the multi-wave LED tip. (C) Beam profile of the multi-wave LED with the 460 ± 10 nm bandpass filter showing the spectral emission pattern nearly within the blue wavelength range (420-495 nm). The black dashed circle area (----) represents the position, orientation and area of the specimen onto the multi-wave LED tip.*

Figure 2A,B show color-coded maps representing, in every 0.5 mm in width and depth, the mean of the degree of conversion (DC, in %) for CQ-amine [A] and CQ-amine/TPO [B] BFCs according to the LED emission position, violet (380-420 nm) and blue (420-495 nm), in width and in depth. The black dashed line in Figure 2A.B represents the limit boundary where at least 80% of the maximum DC on the top of the restoration was achieved by the BFCs. Figure 2C,D shows areas in yellow where significant

Table 3: *Mean ± SD Irradiance (mW/cm²) and Light Transmittance (%) Through CQ-amine and CQ-amine/TPO Bulk-fill Composites in Different Thicknesses Within Violet (380-420 nm) and Blue (420-495 nm) Wavelength Ranges*[a]

	Thickness (mm)	**CQ-amine**		**CQ-amine/TPO**	
		Irradiance (mW/cm²)	**Transmittance** (%)	**Irradiance** (mW/cm²)	**Transmittance** (%)
Violet (380-420 nm)	0	171.0±5.6	100 Aa	171.0±5.6	100 Aa
	1	71.3±5.8	42 Ab	43.8±1.3	26 Bb
	2	38.3±0.3	22 Ac	30.4±1.6	18 Ab
	3	3.6±2.1	2 Ad	0.0±0.0	0 Ac
	4	0.0±0.0	0 Ad	0.0±0.0	0 Ac
	5	0.0±0.0	0 Ad	0.0±0.0	0 Ac
	6	0.0±0.0	0 Ad	0.0±0.0	0 Ac
Blue (420-495 nm)	0	980.0±21.0	100 Aa	980.0±21.0	100 Aa
	1	398.1±25.8	41 Bb	449.4±3.7	46 Ab
	2	257.9±1.8	26 Ac	237.0±1.3	24 Ac
	3	172.6±1.9	18 Ad	170.8±6.0	17 Ad
	4	123.1±1.5	13 Ae	120.7±5.7	12 Ae
	5	77.8±1.5	8 Af	77.5±1.9	8 Af
	6	54.0±2.6	6 Af	55.5±3.0	6 Af

Abbreviations: CQ, camphorquinone; TPO, diphenyl(2,4,6-trimethylbenzoyl) phosphine oxide.
[a] *Post hoc Tukey test* (α=0.05): For each wavelength range (blue or violet), capital letters compare means between photoinitiator systems (CQ-amine and CQ-amine/TPO) and lowercase letters compare means between thicknesses (0, 1, 2, 3, 4, 5, 6 mm).

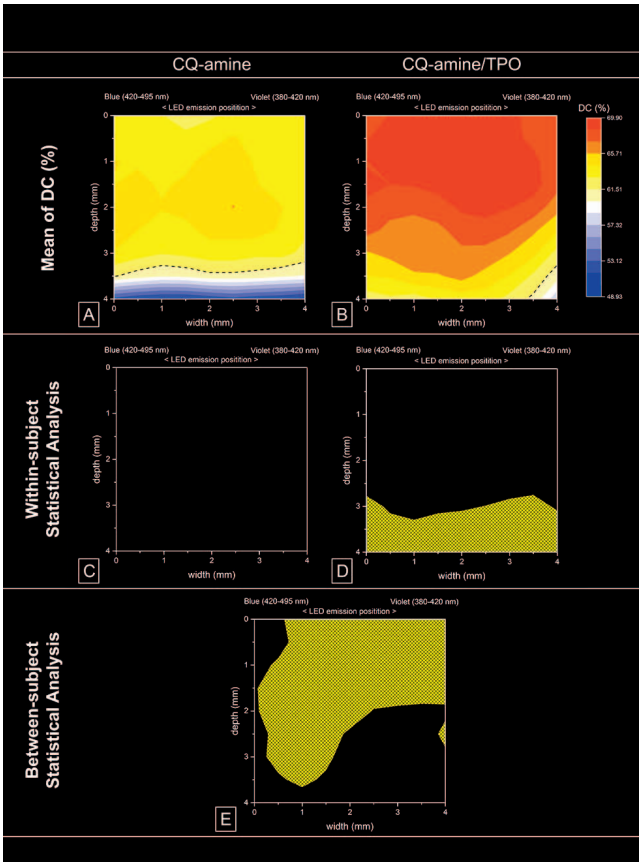

Figure 2. *Curing profile of the mean of the degree of conversion (DC, in %) of CQ-amine (A) and CQ-amine/TPO (B) BFCs according to the LED emission position, violet (380-420 nm) and blue (420-495 nm), in width and depth. The black dashed line (----) in the graphs (A) and (B) represents the limit boundary of 80 % of the maximum DC achieved by the BFCs. Panels (C) and (D) show areas in yellow where significant statistical differences were found within subjects (width and depth nested inside each BFX, CQ-amine or CQ-amine/TPO). Panel (E) shows areas in yellow where significant statistical differences were found in the same position (in width and depth) between subjects (CQ-amine and CQ-amine/TPO bulk-fill composites).*

statistical differences were found within subjects (width and depth nested inside each BFC, CQ-amine or CQ-amine/TPO). The CQ-amine BFC had a homogeneous DC distribution across the specimen since no statistical differences were found between width and depth regions (degrees of freedom [*df*][125]; F=1.03, p=0.409). In contrast, the CQ-amine/TPO BFC had a nonhomogeneous DC distribution across the specimen since statistical differences were found between width and depth regions (*df*([25]; F=1.69, $p<0.001$), where the areas in yellow showed lower DC than the areas in the top part of the specimen. Figure 2E shows areas where significant statistical differences were found between subjects (for the same width and depth position, differences between CQ-amine and CQ-amine/TPO BFCs). In the areas presented in yellow, the CQ-amine/TPO BFC had higher DC than the CQ-amine BFC (*df*[279]; F=30.4, $p<0.001$)

Table 4 shows the results of VS (%), PSS (MPa), rPSS (MPa.s^{-1}), and FM (GPa) for each BFC. There was no statistical difference between CQ-amine and CQ-amine/TPO BFCs for VS (*df*[1]; F=1.23, p=0.310). However, the CQ-amine/TPO BFC had a higher PSS (*df*[1]; F=13.08, p=0.011), rPSS (*df*[1]; F=35.98, p=0.001), and FM (*df*[1]; F=6.86, p=0.020) than the CQ-amine BFC.

DISCUSSION

It is believed that LT through a resin-based composite is a result of photoinitiator absorption, surface reflection, light scattering, and refraction caused by differences in the refractive indexes of monomers and filler particles.[22] As the same monomers and filler concentrations were used for both experimental BFCs, the present study was designed to determine the effect of two photoinitiator systems in the LT properties of the experimental BFCs. The photoinitiator systems used were CQ-amine, which absorbs light in the blue wavelength range from 420 nm to 495 nm with a peak absorption at 470 nm, and CQ-amine/TPO, which absorbs light in the violet and blue wavelength range from 350 nm to 495 nm with two peak absorptions at 380 and 470 nm.[15] Since several lines of evidence suggest a strong relationship between the spectral output of the light curing unit and the photoinitiator absorption,[6,22,23] the multi-wave LED used to light cure the BFCs emitted 20 J/cm^2 of radiant exposure and covered photoinitiator absorption of both CQ-amine and CQ-amine/TPO BFCs.

However, differences were found between the violet and blue wavelength emissions for the multi-wave LED. While 16.6 J/cm^2 was emitted into the blue spectrum, only 3.4 J/cm^2 was emitted into the violet spectrum. Nevertheless, despite the differences in the amount of violet and blue light emitted by the multi-wave LED, previous evidence presented thus far supports the idea that the spectral output of the multi-wave LED used was enough to efficiently cure BFCs containing either CQ-amine or CQ-amine associated with alternative photoinitiators.[6,10,16,26] The present study findings are in agreement with those of previous studies; however these conclusions should be interpreted with further attention since they do not rule out the influence of other factors, such as, the light beam profile received by the specimen.

Table 4: *Mean ± SD and One-way ANOVA Results of VS, PSS, rPSS, and FM of CQ-amine and CQ-amine/TPO Bulk-fill Composites*

	CQ-amine	CQ-amine/TPO	One-way ANOVA (α=0.05; β=0.20)
VS (%)	2.20±0.15	2.30±0.17	*df*(1); F=01.23, p=0.310
PSS (MPa)	2.94±0.07	3.82±0.48	*df*(1); F=13.08, p=0.011
rPSS (MPa.s^{-1})	0.34 ±0.02	0.70±0.12	*df*(1); F=35.98, p=0.001
FM (GPa)	7.37±0.76	8.46±0.88	*df*(1); F=06.86, p=0.020

Abbreviations: ANOVA, analysis of variance CQ, camphorquinone; df, degrees of freedom; FM, flexural modulus; PSS, polymerization shrinkage stress; rPSS, maximum rate of polymerization shrinkage stress; TPO, diphenyl(2,4,6-trimethylbenzoyl) phosphine oxide; VS, volumetric shrinkage.

Therefore, a note of caution is due here since the beam profile results are in accordance with recent studies indicating that the light distribution throughout the multi-wave LED bluephase G2 light tip is significantly influenced by the reflectors, LED chip positions, and the presence of three blue LED chips and only one violet LED chip.[24,25] Then, the most recognizable finding to emerge from the light curing unit characterization is that the light received on the top surface of the specimens used in this study was not homogeneously distributed, neither in irradiance nor in wavelength. Consequently, the key problem with the nonhomogenous light emission is that it might have important implications for the degree of conversion homogeneity throughout the entire BFC restoration.

But it is somewhat interesting that this is not true for all case scenarios, and the data reported here appear to support the assumption that CQ-amine and CQ-amine/TPO BFCs would have different behaviors regarding the degree of conversion homogeneity when light cured with a nonhomogeneous dual-peak multi-wave LED. To some degree, the CQ-amine BFC had a lower overall DC than the CQ-amine/TPO BFC, but it was homogeneously distributed across the entire specimen. In contrast, the CQ-amine/TPO BFC had a higher overall DC than the CQ-amine BFC, but there were differences between the top and bottom part of the specimen.

It is therefore likely that such connections exist between the position of the violet light beam and the presence of TPO. As shown in Figure 2E, the DC of the CQ-amine/TPO BFC was equal or higher than the DC of the CQ-amine BFC, and this discrepancy is more pronounced in areas where there is an overlap between violet and blue light. But the fact is that the presence of TPO has a significant influence on the DC. TPO is known as a high reactive photoinitiator because it has a higher molar extinction coefficient (≈520 L/mol cm) than CQ (≈28 L/mol cm). This means that TPO absorbs light more efficiently than CQ at their peak wavelength absorptions[27] and that TPO cleavage forms acyl (carbon centered) and phosphonyl (phosphorus centered) free radicals that have higher nucleophilicity and electron resonance than the amino radical (carbon centered) formed by CQ-amine electron donor/hydrogen abstraction reaction, Thus, initiation of polymerization is increased, leading to a higher DC.[27]

Although these differences in the DC are strictly related to the top part of the restoration due to the TPO wavelength absorption within the violet wavelength range, previous studies have shown that the DC of a polymer-based composite is related to its RI.[13] Consequently, it is expected that the polymer network with a higher DC formed by the same monomers would have a higher refractive index, closing the mismatch between polymer and filler refractive indexes and improving the LT. As shown in Table 4, the CQ-amine/TPO BFC has a higher blue LT than the CQ-amine BFC, but, contrary to expectations, this difference was found up to 1 mm in thickness, meaning that the improvement in the DC was not enough to improve the blue LT through the BFC. Therefore, the first research hypothesis tested—that the combination of CQ and TPO will increase the depth of cure of BFCs—was rejected.

Nevertheless, a higher DC on the top of the restoration might improve the wear and hydrolytic degradation resistance and perhaps the clinical performance of BFC.[28] Therefore, it can thus be suggested that the combination of CQ-amine and TPO would improve chemical and physical properties of BFCs. However, in a more systematic approach this study also identified how CQ-amine and TPO interact with PSS.

Despite no statistical differences being found between the CQ-amine and CQ-amine/TPO BFCs regarding the VS, the combination of CQ and TPO increased the rPSS, PSS, and FM. For CQ-based composites, it is necessary to use an amine together with the CQ to form free radicals efficiently enough to initiate polymerization[5]; however, when CQ and amine are combined with TPO, the reaction could

increase autoacceleration (Trommsdorff-Smith effect).[29,30]

The major issue is the presence of a tertiary amine (ie, EDMAB) combined with TPO, especially because acyl and phosphonyl radicals formed by TPO cleavage can abstract a hydrogen atom from a tertiary amine, creating one more way to initiate polymerization. This reaction is so fast that it could accelerate the rate of polymerization and the vitrification of the polymer. This means that a very fast reaction does not provide enough time to relax the internal structure, and this shrinkage stress is transferred to the tooth's boundaries.[31]

Furthermore, the stiffness of the material affects the stress produced as a result of polymerization.[31,32] According to Hook's law, FM = Stress/Strain, and because the flexural modulus represents the ratio of the elastic stress to the elastic strain, it follows that the higher the stress for a given strain, the higher the FM can be a factor for the higher PSS of CQ-amine/TPO BFC. Therefore, the second research hypothesis tested—that the combination of CQ and TPO will increase polymerization shrinkage stress of BFCs—was accepted.

Recent evidence suggests that the effect of combining CQ-amine and TPO at a molar ratio of 1:1 can improve optical properties without reducing the depth of cure of conventional composites.[15] What is surprising is that perhaps the most serious consequences of combining CQ-amine and TPO are related to PSS and, thus, the clinical performance of BFCs containing CQ-amine and TPO.

Nevertheless, the lack of clinical evidence could lead to a concern regarding the combination of these two photoinitiator systems in BFCs. Bayraktar and others[11] showed that a composite containing CQ-amine associated with alternative photoinitiators (TPO and Ivocerin) has a higher incidence of discontinued anatomic form, marginal discoloration, creviced in which dentin is exposed, and secondary caries than a composite containing only CQ-amine in just one year of observation.[11] But certainly, this should be observed with more caution because from 50 restorations placed using the composite containing CQ-amine with alternative photoinitiators in this study, only two restorations failed, which means that other factors, such as operator technique, especially during the light curing procedure, might be the cause of these failures. Still, this study seems to have overlooked one important fact that the light curing unit used to cure the CQ-amine with alternative photoinitiators composites was a single peak blue spectrum monowave LED (Elipar S10, 3M ESPE, St Paul, MN, USA). As the monowave LED used has a single peak emission at 450 nm[24] and the BFC used contains TPO and Ivocerin phoinitiators with peak absorption at 370 nm and 418 nm. respectively,[6] it seems possible that these negative results are due to poor composite light curing.

In addition, Schwendicke and others[33] published a very robust meta-analysis showing the clinical performance of directly placed restorative materials. In that study, 72 randomized controlled trials published between 2005 and 2015 were selected; however, only 8 studies included BFCs. Moreover, only 3 studies were using high-viscosity BFC and none of them included BFCs with alternative photoinitiators. Given that most clinical trials analyzed were short term and showed high risk of bias, future clinical trials should focus on comparative designs and reports using materials with the same composition but different photoinitiator systems.

It is almost certain that the polymerization reaction produces stress that would not be adequately dissipated by the strain caused within the composite, even in BFCs. Therefore, it is probable that the stress is transferred to the bonded interfaces with the tooth structure creating delamination or tooth fracture whenever and wherever the localized stress exceeds the adhesion strength or the strength of the adjacent residual tooth structure. Furthermore, these stresses may increase with time, causing delayed damage to cavity margins. Although many studies have shown *in vitro* evidence of marginal failures using commercially available BFCs, there is abundant room for further progress determining systematically the connections between the combination of photoinitiators and the marginal failures in experimental materials. The findings in this study indicate that CQ-amine/TPO BFCs could have a higher PSS than CQ-amine BFCs. This suggests that a weak link may exist between PSS and the marginal adaptation of BFCs containing CQ-amine associated with TPO.

Nevertheless, new alternatives to improve light curing of BFCs have emerged. Oliveira and others[34] showed new composites containing photoinitiators systems that light cured using longer wavelength range (green or red light) than short wavelength range (violet or blue). Apparently, long wavelengths have higher light transmittance than short wavelengths, but further work is required to establish the viability of using these high-efficiency photoinitiators to improve the depth of cure of BFCs. Still, the use of high-reactive photoinitiators in a BFC might

be a drawback since they could increase PSS unless the stress-relief monomer system could compensate for the increasing PSS caused by these photoinitiators. However, recent studies concerning the development of new monomer systems based on thiol-ene polymerization reactions (thio-urethanes)[17] might be a promising alternative to reduce the PSS of BFCs.

CONCLUSION

Within the limitations of this study, the following conclusions can be made: Although the CQ-amine/TPO BFC has a higher DC on the top of the restoration, the combination of CQ-amine and TPO could not increase the blue light transmission to enhance the depth of cure of BFCs. Also, despite the CQ-amine/TPO BFC having some improvement in mechanical properties, such as FM, the CQ-amine/TPO BFC had a higher PSS and rPSS than the CQ-amine BFC.

Acknowledgements

This study was supported by the FAPESP (grant #2016/06019-3 and #2017/22195-9). Dayane Carvalho Ramos Salles de Oliveira is a postdoctoral researcher at FAPESP (grant #2016/05823-3 and #2017/22161-7). We would like to acknowledge Esstech and Evonik for the kind donation of the materials used in this study.

Conflict of Interest

The authors of this manuscript certify that they have no proprietary, financial, or other personal interest of any nature or kind in any product, service, and/or company that is presented in this article.

(Accepted 7 October 2018)

REFERENCES

1. Kim RJ, Kim YJ, Choi NS, & Lee IB (2015) Polymerization shrinkage, modulus, and shrinkage stress related to tooth-restoration interfacial debonding in bulk-fill composites *Journal of Dentistry* **43(4)** 430-439.
2. Issa Y, Watts DC, Boyd D, & Price RB (2016) Effect of curing light emission spectrum on the nanohardness and elastic modulus of two bulk-fill resin composites *Dental Materials* **32(4)** 535-550.
3. AlQahtani MQ, Michaud PL, Sullivan B, Labrie D, AlShaafi MM, & Price RB (2015) Effect of high irradiance on depth of cure of a conventional and a bulk fill resin-based composite *Operative Dentistry* **40(6)** 662-672.
4. Vivadent I (2014) Tetric EvoCeram® Bulk Fill simplifies composite restoration placement, increases efficiency *Compendium of Continuing Education in Dentistry* **35(6)** 432.
5. Neumann MG, Schmitt CC, Ferreira GC, & Correa IC (2006) The initiating radical yields and the efficiency of polymerization for various dental photoinitiators excited by different light curing units *Dental Materials* **22(6)** 576-584.
6. Rocha MG, De Oliveira DCRS, Correa IC, Correr-Sobrinho L, Sinhoreti MAC, Ferracane JL, & Correr AB (2017) Light-emitting diode beam profile and spectral output influence on the degree of conversion of bulk fill composites *Operative Dentistry* **42(4)** 418-427.
7. Shortall AC, Palin WM, & Burtscher P (2008) Refractive index mismatch and monomer reactivity influence composite curing depth *Journal of Dental Research* **87(1)** 84-88.
8. de Oliveira DC, de Menezes LR, Gatti A, Correr Sobrinho L, Ferracane JL, & Sinhoreti MA (2016) Effect of nanofiller loading on cure efficiency and potential color change of model composites *Journal of Esthetic and Restorative Dentistry* **28(3)** 171-177.
9. Campos EA, Ardu S, Lefever D, Jasse FF, Bortolotto T, & Krejci I (2014) Marginal adaptation of class II cavities restored with bulk-fill composites *Journal of Dentistry* **42(5)** 575-581.
10. Fronza BM, Rueggeberg FA, Braga RR, Mogilevych B, Soares LE, Martin AA, Ambrosano G, & Giannini M (2015) Monomer conversion, microhardness, internal marginal adaptation, and shrinkage stress of bulk-fill resin composites *Dental Materials* **31(12)** 1542-1551.
11. Bayraktar Y, Ercan E, Hamidi MM, & Colak H (2017) One-year clinical evaluation of different types of bulk-fill composites *Journal of Investigative and Clinical Dentistry* **8(2)**
12. Rocha MG, Oliveira DCRS, Correr AB, & Sinhoreti MAC (2017) Dental bulk-fill composite and use thereof *World Intellectual Property Organization* WO2017181252.
13. Hadis MA, Tomlins PH, Shortall AC, & Palin WM (2010) Dynamic monitoring of refractive index change through photoactive resins *Dental Materials* **26(11)** 1106-1112.
14. Ogunyinka A, Palin WM, Shortall AC, & Marquis PM (2007) Photoinitiation chemistry affects light transmission and degree of conversion of curing experimental dental resin composites *Dental Materials* **23(7)** 807-813.
15. de Oliveira DCRS, Rocha MG, Correa IC, Correr AB, Ferracane JL, & Sinhoreti MAC (2016) The effect of combining photoinitiator systems on the color and curing profile of resin-based composites *Dental Materials* **32(10)** 1209-1217.
16. Li X, Pongprueksa P, Van Meerbeek B, & De Munck J (2015) Curing profile of bulk-fill resin-based composites *Journal of Dentistry* **43(6)** 664-672.
17. Faria ESAL & Pfeifer CS (2017) Impact of thio-urethane additive and filler type on light-transmission and depth of polymerization of dental composites *Dental Materials* **33(11)** 1274-1285.
18. Pfeifer CS, Ferracane JL, Sakaguchi RL, & Braga RR (2008) Factors affecting photopolymerization stress in dental composites *Journal of Dental Research* **87(11)** 1043-1047.
19. Watts DC & Satterthwaite JD (2008) Axial shrinkage-stress depends upon both C-factor and composite mass *Dental Materials* **24(1)** 1-8.

20. Watts DC, Marouf AS, & Al-Hindi AM (2003) Photopolymerization shrinkage-stress kinetics in resin-composites: methods development *Dental Materials* **19(1)** 1-11.
21. Muench A, Correa IC, Grande RH, & Joao M (2005) The effect of specimen dimensions on the flexural strength of a composite resin *Journal of Applied Oral Science* **13(3)** 265-268.
22. Hadis MA, Shortall AC, & Palin WM (2012) Competitive light absorbers in photoactive dental resin-based materials *Dental Materials* **28(8)** 831-841.
23. Shimokawa C, Sullivan B, Turbino ML, Soares CJ, & Price RB (2017) Influence of emission spectrum and irradiance on light curing of resin-based composites *Operative Dentistry* **42(5)** 537-547.
24. Shortall AC, Felix CJ, & Watts DC (2015) Robust spectrometer-based methods for characterizing radiant exitance of dental LED light curing units *Dental Materials* **31(4)** 339-350.
25. Price RB, Labrie D, Rueggeberg FA, & Felix CM (2010) Irradiance differences in the violet (405 nm) and blue (460 nm) spectral ranges among dental light-curing units *Journal of Esthetic and Restorative Dentistry* **22(6)** 363-377.
26. Fronza BM, Ayres A, Pacheco RR, Rueggeberg FA, Dias C, & Giannini M (2017) Characterization of inorganic filler content, mechanical properties, and light transmission of bulk-fill resin composites *Operative Dentistry* **42(4)** 445-455.
27. Neumann MG, Miranda WG Jr, Schmitt CC, Rueggeberg FA, & Correa IC (2005) Molar extinction coefficients and the photon absorption efficiency of dental photoinitiators and light curing units *Journal of Dentistry* **33(6)** 525-532.
28. Ferracane JL (2013) Resin-based composite performance: are there some things we can't predict? *Dental Materials* **29(1)** 51-58.
29. Gooch JW (2011) *Autoacceleration. Encyclopedic Dictionary of Polymers* Springer, New York NY 55-56.
30. O'Shaughnessy B & Yu J (1994) Autoacceleration in free radical polymerization. 1. Conversion *Macromolecules* **27(18)** 5067-5078.
31. Kalliecharan D, Germscheid W, Price RB, Stansbury J, & Labrie D (2016) Shrinkage stress kinetics of bulk fill resin-based composites at tooth temperature and long time *Dental Materials* **32(11)** 1322-1331.
32. Park JH & Choi NS (2017) Equivalent Young's modulus of composite resin for simulation of stress during dental restoration *Dental Materials* **33(2)** e79-e85.
33. Schwendicke F, Göstemeyer G, Blunck U, Paris S, Hsu LY, & Tu YK (2016) Directly placed restorative materials: Review and network meta-analysis *Journal of Dental Research* **95(6)** 613-622.
34. Oliveira D, Rocha M, Correr A, Silvino A, & Sinhoreti M (2017) From blue to red: New photoinitiator systems for dental materials *Dental Materials* **(33)** e88-e89.